PAPER SUBMITTED FOR TRANSPORTATION RESEARCH RECORD (TRR), JOURNAL OF TRANSPORTATION RESEARCH BOARD
DECEMBER 2012

Urban route average travel time estimation considering exit turning movements

Ashish Bhaskar*
School of Urban Development
Queensland University of Technology
Brisbane, Australia
Ph: +61 7 3138 9985
Fax: +61 3138 1827
ashish.bhaskar@qut.edu.au

Prof. Edward Chung
School of Urban Development
Queensland University of Technology
Brisbane, Australia
Ph: +61 7 31381143
Fax: +61 3138 1827
edward.chung@qut.edu.au

Prof. André-Gilles Dumont
Laboratory of Traffic Facility
Swiss Federal Institute of Technology
Lausanne, Switzerland
Ph: +41 21 693 2345
Fax: +41 21 693 63 49
andre-gilles.dumont@epfl.ch

*Corresponding Author

Number of Words in the Text	4450
Number of Figures in the Text	12(=3000 words)
Total Equivalent Words	7450

ABSTRACT

This paper presents a methodology for real-time estimation of exit movement specific average travel time on urban routes by integrating real-time cumulative plots, probe vehicles and historical cumulative plots. Two different approaches, *Component* based and *Extreme* based are discussed for route travel time estimation. The methodology is tested using simulation and validated with real data (from Luzern, Switzerland) that demonstrates its potential for accurate estimation. Both approaches provide similar results. The *Component* based approach is more reliable with a greater chance of obtaining a probe vehicle in each interval, though additional data from each component is required. The *Extreme* based approach is simple, and only requires data from upstream and downstream of the route, but the chances of obtaining a probe that traverses the entire route might be low. The performance of the methodology is also compared with a method solely based on probe (*Probe-Only*). The proposed methodology requires only a small number of probes for accurate estimation, whereas *Probe-Only* requires a significantly larger number of probes.

***Keywords*:** Movement specific travel time, Urban route travel time, Cumulative plots, Probe, Data fusion.

1 INTRODUCTION

Travel time is the time needed to travel from point upstream (*u/s*) to point downstream (*d/s*) on the network. It is an important network performance measure and it quantifies congestion in a manner easily understood by all transport users. Travel time estimation has been researched for many years, with most of the literature focusing on freeways [1-3]. Urban network travel time estimation is challenging for various reasons including external control of traffic using signals, non-conservation of traffic on urban links (due to parking etc.), significant differences in travel time for different exit turning movements, and etc.

Loop detectors are the oldest and most widely used traffic data sources and hence, the majority of traffic models are based on detector data. Researchers have proposed a number of models with various degrees of complexity ranging from simple volume delay functions [4-14], regression analysis-based [15-20], to applied machine learning algorithms [21-23] for urban network travel time estimation.

Mobile sensors such as probe vehicles are equipped with vehicle tracking equipment (e.g. taxi fleet with GPS) and can provide data for a vehicle's trajectory (time stamp and position coordinates) and hence its travel time. Probes represent a random sample from the population of the vehicles traversing the link. Therefore, the average travel time of all vehicles traversing the link can be estimated by statistical sampling techniques [24, 25]. Researchers [25, 26] have shown interest in determining the minimum number of probes required for statistically significant travel time estimation.

Researchers have also applied data fusion techniques [27-31] to fuse data from different sources, specifically detector and probe vehicles, with the aim of improving the accuracy and reliability of the estimates.

An urban route can consist of a number of intersections. The flow on an urban link between two consecutive signalized intersections can be from different entrance links upstream, towards different exit links downstream (For instance, in Figure 1*a*, there are nine different combinations of flows such as, A→Lft, B→Lft, etc.) and based on the delay experienced by the vehicle at the intersections, the travel time for these combinations may be different. For route travel time estimation one is interested in one of these combinations based on the flow associated with the route. Figure 1*b* is a real, individual vehicle travel time for two different exit movements on one of the urban signalised links.

It can be seen that travel time from *u/s* to *Lft* movement (thin black line) is significantly higher than that from *u/s* to *Thru* movement (thick grey line). Average link travel time (thick black line) is not a true representative of different movements. Hence, it is worth analysing travel time for different movements associated with the link. Moreover, movement specific travel time provides a detailed understanding of the network performance. For instance, excessive travel time for an exit movement can identify the critical movement at an intersection. The aforementioned literature is limited to the average link travel time estimation, and generally to estimate movement specific link travel time, penalties are added to the average link travel time. The considered penalties are static, whereas in reality they are dynamic and are correlated with the downstream link performance (for instance a spill back from the downstream link restricts the entry flow). Therefore, the existing approach of using penalties cannot capture the dynamics of real traffic and can result in significant errors in movement specific estimation. The objective of this paper is to define an accurate and robust methodology for movement specific link average travel time estimation and apply it to route travel time estimation.

Initially, the methodology for movement specific link travel time estimation is discussed. Then two different approaches for route travel time are discussed. Finally, the result of testing and validation are presented.

2 METHODOLOGY

2.1 Exit movement Specific Travel Time

The classical analytical procedure for travel time estimation is based on defining cumulative plots (cumulative counts of vehicles versus time) U(t) and D(t) at upstream and downstream locations, respectively [32]. Refer to Figure 2*a*, if vehicles represented in U(t) between time from t_1 to t_2; and D(t) between time from t_3 to t_4, are same then area, *A*, between the plots is the total travel time and the average travel time $\overline{TT}$ within an estimation interval T_{EI} (= $t_4 - t_3$) is as follows:

$$\overline{TT} = \frac{A}{N} = \frac{\sum_{i=1}^{N}\left[D^{-1}(i) - U^{-1}(i)\right]}{N} = \frac{\sum_{i=1}^{N} D^{-1}(i) - \sum_{i=1}^{N} U^{-1}(i)}{N} \quad (1)$$

where: $N = U(t_2) - U(t_1) = D(t_4) - D(t_3)$

Here *N* is the number of vehicles that depart downstream (arrives upstream) during the time t_3 to t_4 (t_1 to t_2).

The classical procedure is vulnerable to the relative deviations (RD) amongst the plots and in urban networks there are potential sources of RD such as mid-link sources/sinks, and detector counting errors etc. For instance, if an upstream detector is undercounting (*see* Figure 2*b*), then both U(t) and D(t) can cut each other and the classical procedure cannot be applied. Bhaskar et al., [33] have developed a methodology named CUmulative plots and PRobe Integration for Travel timE estimation (CUPRITE) by integrating cumulative plots and probe vehicle data to address the issues related to RD. In this paper, we extend the methodology to consider different exit movements at *d/s* and estimate route travel time based on two different approaches: *Component* based and *Extreme* based. The following subsections explain issues concerned with the estimation of movement specific travel time (section 2.1.1) and introduce the architecture (section 2.1.2) and detailed explanation (sections 2.1.3 to 2.1.5) of the proposed methodology. The approaches for route travel time are presented in section 2.2.

2.1.1 Issue

Say, for an urban link, $U_m(t)$ and $D_m(t)$ are upstream and downstream cumulative plots for m^{th} exit movement, respectively; $U_T(t)$ (2) is the cumulative plot based on total flow from the upstream links (Refer to Figure 1*a*: *m* = Lft, Thru and Rt and U_T is the cumulative plot at u/s based on the flow from A, B and C).

$$U_T(t) = \sum_{\forall m} U_m(t) + \varepsilon \qquad (2)$$

Where ε are the counts associated with mid-link sink, error in detector counting, etc.

If $U_m(t)$ and $D_m(t)$ are known then the classical procedure can be applied for estimation travel time for m^{th} downstream exit-movement. Assuming detectors are at the stop-line, **$D_m(t)$ and $U_T(t)$ can be obtained, whereas $U_m(t)$ is unknown**. If we have probe data then $U_m(t)$ is defined by integrating $U_T(t)$, $D_m(t)$ and probe data (Section 2.1.4). However, probe data is not always available, at least for different estimation periods in real time. To address this issue we propose a hybrid technique where we use historical effective scaling factors to define $U_m(t)$ from $U_T(t)$ (Section 2.1.5).

For simplicity of discussion we use the term exit moment. To be precise we consider the combination of different movements, based on link geometry and signal phases. For instance: for *d/s* in Figure 1*c*, travel time for all the movements is independently considered ($D_{Rt}(t)$, $D_{Lft}(t)$, and $D_{Thru}(t)$ are obtained from detector d_1, d_2, and d_3, respectively), whereas, for *d/s* in Figure 1*d*, through and left movements are jointly considered ($D_{Rt}(t)$ and $D_{Thru+Lft}(t)$ are obtained from detector d_4 and sum of counts from detectors d_5 and d_6, respectively).

2.1.2 Architecture

The proposed architecture of CUPRITE for exit movement specific travel time estimation is presented in Figure 3. The following steps are involved:

- Step 1 $U_T(t)$ and $D_m(t)$ are estimated. If detector data is pulse data (vehicle data), then cumulative plots are obtained by cumulating the pulses. If detector data is aggregated data (say counts every one minute) then detector data is integrated with signal timings, where counts during the signal red phase time are assigned as zero and counts during signal green phase time are segregated into saturation flow rate and non saturation flow rate. Refer to [34] for the integration of detector counts and signal timings for accurate estimation of cumulative plots.
- Step 2 Initial estimate of $U_m(t)$ is obtained by applying *vertical scaling* on $U_T(t)$ (Section 2.1.3);
- Step 3 If probe data is available then the *points from where $U_m(t)$ should pass* are defined and $U_m(t)$ is redefined by applying *vertical scaling* on it (Section 2.1.4). Here, iff the link has no mid-link delay (such as mid-link intersection, or bus stop) and the system is undersaturated, one can consider virtual probes [33] i.e. virtual vehicles with travel time as freeflow link travel time, and departing *d/s* at the end of signal green phase time.
- Step 4 Apply the classical procedure (1) between redefined $U_m(t)$ and $D_m(t)$ to estimate average movement specific travel time.

2.1.3 Initial Estimate of $U_m(t)$

Say variables: *d*, *p*, and *m*, represent days of the week, time periods during the day, and m^{th} exit turning movement, respectively; $S_{m,p,d}$ represents the scaling factor for m^{th} exit movement, p^{th} period

of d^{th} day of the week (e.g., $S_{Lft,7:00–7:15am,Monday}$ is the scaling factor for left exit movement, from 7:00 to 7:15 on Monday); and $t_{e,p}$ and $t_{s,p}$ is the time corresponding to the start and end of the p^{th} average travel time estimation time period, respectively. The default value of $S_{m,p,d}$ is 1.0 (It could also be assigned to the expected average proportion of link flow for the respective exit movement.). **In Section 2.1.5 we will discuss how $S_{m,p,d}$ is defined by using an historical database.**

Initial estimate for $U_m(t)$ (Figure 4*a*) is obtained by vertical scaling $U_T(t)$ with respective scaling factor $S_{m,p,d}$ for each time period (3). First, $U_m(t=0) = U_T(t=0)$. Thereafter, counts for the movement m during each time period are estimated and $U_m(t)$ is obtained by cumulating the estimated count, as explained below:

$$\forall \, Time\ Periods\ and\ \forall\, t \in [t_{s,p},\ t_{e,p}]$$

$$Y(t) = S_{m,p,d}[U_T(t) - U_T(t_{s,p})] \qquad (3)$$

$$U_m(t) = U_m(t_{s,p}) + Y(t)$$

Here, for any time *t* between time $t_{s,p}$ and $t_{e,p}$:

$Y(t)$ is the count for the movement m from time $t_{s,p}$ to time t;

$U_T(t) - U_T(t_{s,p})$ is the count from total cumulative plot from time $t_{s,p}$ to time t;

$S_{m,p,d}$ $[U_T(t) - U_T(t_{s,p})]$ are scaled count for the movement m from time $t_{s,p}$ to time t;

$U_m(t_{s,p})$ is the cumulative count for movement m at time $t_{s,p}$;

$U_m(t)$ is obtained by cumulating the estimated counts $Y(t)$.

The above process is repeated for each time periods.

Note: If $S_{m,p,d}$ =1 then, $U_m(t) = U_T(t)$.

2.1.4 If Probe Data is Available: $U_m(t)$ is estimated by integrating probe data with cumulative plots

Here, the probe vehicle is the vehicle which provides a time stamp when at the intersection (position where cumulative plots are generated). There are issues related to probe data such as frequency of data, map-matching of data, etc. Addressing such issues is beyond the scope of this paper. We assume that the known value of time, t_u and t_d when a probe vehicle is at upstream and downstream intersection, respectively.

Given the probe data, we fix the probe to $D_m(t)$ i.e., assign its rank in cumulative plots as $D_m(t_d)$. Thereafter, we *define points from where $U_m(t)$ should pass* and finally apply *vertical scaling* on the initial estimate of $U_m(t)$ to redefine $U_m(t)$ as explained below.

Say we have n probe vehicles and the database for the probe is defined as lists of $[t_u]$ and $[t_d]$ where the size of each list is n. The value of j^{th} element in the list represents the data from the j^{th} probe. The following steps *define the points from where $U_m(t)$ should pass*:

Step 1 Sort list $[t_d]$ in ascending order of its values. This is required as the rank of the probe in the cumulative plots is defined based on $D_m(t)$.

Step 2 Sort list $[t_u]$ in ascending order of its values in order to make sure that the redefined $U_m(t)$ is monotonically increasing.

Step 3 The required points through which $U_m(t)$ should pass are $(t_{uj}, D(t_{dj}))$; where t_{uj} and t_{dj} are j^{th} value in the sorted list of $[t_u]$ and $[t_d]$, respectively.

$U_m(t)$ and $D_m(t)$ were initially two independent cumulative plots. When the traffic condition is free-flow (say at time t_0 = 1:00 am) then counts for cumulative plots can be initialised to zero ($U_m(t_0) = D_m(t_0)=0$). This is the initial reference point (P_0). Say $[P_1, P_2, P_3, \ldots, P_n]$ is the list of *n* points from where $U_m(t)$ should pass, then for redefining $U_m(t)$ for point P_i, the reference point is P_{i-1}.

Say we have: a) a reference point (t_{Ref}, $U_m(t_{Ref})$), i.e., the point in which we have confidence that it is the correct point on the plot; and b) point (t_p, Y_p) through which $U_m(t)$ should pass. Then (refer to equations(4), (5) and (6) and Figure 4*b*) we redefine $U_m(t)$ by applying a correction to it such that all points on the plot:

1) Before time t_{Ref} have no correction;
2) Between t_{Ref} and t_p are scaled vertically; and
3) Beyond t_p are shifted vertically so that the redefined $U_m(t)$ is continuous at time t_p and is parallel to $U_m(t)$.

$$U_m(t) = U_m(t) + Correction \tag{4}$$

$$Correction = \begin{cases} 0 & \forall\ t \le t_{Ref} \\ (scale-1)*(U_m(t) - U_m(t_{\text{Ref}})) & \forall\ t_{Ref} < t < t_p \\ (scale-1)*(U_m(t_p) - U_m(t_{\text{Ref}})) & \forall\ t \ge t_p \end{cases} \tag{5}$$

$$scale = \begin{cases} \dfrac{Y_p - U_m(t_{\text{Ref}})}{U_m(t_p) - U_m(t_{\text{Ref}})} & if\ U_m(t_p) \ne U_m(t_{\text{Ref}}) \\ 1 & if\ U_m(t_p) = U_m(t_{\text{Ref}}) \end{cases} \tag{6}$$

2.1.5 How to Define the Historical Database of Effective Scaling Factor: $S_{m,p,d}$

The redefined $U_m(t)$ with probe data (Section 2.1.4) is used to develop a historical database of effective scaling factors for different times of the day and days of the week. The effective scaling factor incorporates the scaling required for an exit turning ratio and also due to probable loss/gain of vehicles to/from mid-link sinks/sources. To develop the database, at the end of each day $U_T(t)$ and $U_m(t)$ are integrated to define the effective scaling factor for time periods with at least one probe vehicle.

Refer to Figure 5. Say we have a historical database of the effective scaling factor (with the default value of $S_{m,p,d}$ = 1). For each of the periods shown in the figure, first the scaling factor from the historical database is obtained and an initial estimate of $U_m(t)$ from $U_T(t)$ (Section 2.1.3) is defined using equation (3) (Figure 5*a* and *b*) . Thereafter, if probe vehicle data is available, then $U_m(t)$ is redefined as discussed in Section 2.1.4 (Figure 5*c* and *d*) . Finally (Figure 5*e*), for periods using the probe vehicle only, the redefined $U_m(t)$ and $U_T(t)$ are integrated to define the scale $s_{m.p,d}$ (7) for a record of m^{th} exit movement, p^{th} time period of d^{th} day of the week.

$$s_{m,p,d} = \frac{Y_{T,d,p} - Y_{m,d,p}}{Y_{T,d,p}}$$

$$Where: \tag{7}$$

$$Y_{T,d,p} = U_T(t_{e,p}) - U_T(t_{s,p})$$

$$Y_{m,d,p} = U_m(t_{e,p}) - U_m(t_{s,p})$$

Where:

$t_{e,p}$ and $t_{s,p}$ are the time corresponding to the start and end of the p^{th} time period, respectively;
$Y_{T,d,p}$ and $Y_{m,d,p}$ are the counts observed during p^{th} time period in $U_T(t)$ and redefined $U_m(t)$, respectively (see Figure 5*e*).

The historical database is updated with the estimated scale $s_{m.p,d}$. Therefore, the database consists of the values of effective scaling factor $s_{m,p,d}$ properly classified with the corresponding time of the day and day of the week. The database is self-updated daily, with new values defined at the end of the

day as explained above. The required scaling factor $S_{m,p,d}$ (8) is the median of values of effective scaling factor defined in the historical database.

$$S_{m,p,d} = Median\ of\ s_{m,p,d} \quad (8)$$

2.2 Route Travel Time

For route travel time estimation we consider the following two approaches:

2.2.1 Component Based (R_C)

Here we divide the entire route into different components, and the sum of time-slice travel time from each component is route travel time. The component is an exit movement specific link between two consecutive signalised intersections. We consider the pairs of cumulative plots at upstream and downstream for each component. Each pair of cumulative plots is independent from the other pair in the network and RD amongst each pair is corrected independently by applying the methodology explained in section 2.1. Here:

1) $U_{c,m}(t)$ and $D_{c,m}(t)$ represent a pair for m^{th} movement of component (link) c;
2) If we have n components, then c =1,2,3,..,n-1, n where n is the most downstream component and 1 is the most upstream component.
3) We are interested in estimating average travel time for the vehicle that departs the route between time period $t_{s,n}$ to $t_{e,n}$.

Referring to Figure 6*a*, we first investigate the downstream component (n) and define average travel time during the above time period. Then, we look at the time period from $t_{s,n-1}$ to $t_{e,n-1}$ during which the vehicles are observed at the upstream component (n-1) where: $t_{s,n-1}=U^{-1}_{n,m}(D_{n,m}(t_{s,n}))$ and $t_{e,n-1}=U^{-1}_{n,m}(D_{n,m}(t_{e,n}))$, and define the average travel time for all vehicles that depart during time $t_{s,n-1}$ to $t_{e,n-1}$ from component n-1. This process is repeated for further upstream components. The sum of travel times for each component is the route travel time (refer to the example in Figure 6*a*).

2.2.2 Extreme Based (R_E)

Here we estimate route travel time by directly considering the area between the cumulative plots at extreme points of the route i.e., upstream entrance and downstream exit of the route.

To better understand this approach, a self explaining example for R_C and R_E approaches is illustrated in Figure 6, where we are interested in estimating route travel time from point *S* to point *E* (left exit at intersection C). For R_C (Figure 6*a*), three components SA, AB and BC are defined with pairs of cumulative plots ($U_{SA,T}$, $D_{SA,Thru}$), ($U_{AB,T}$, $D_{AB,Thru}$), and ($U_{BC,T}$, $D_{BC,Lft}$), respectively, and where $U_{c,T}$ is the total upstream cumulative plot (2) for component (link) c. For R_E (Figure 6*b*) the pair considered is ($U_{SA,T}$, $D_{BC,Lft}$). Each of these pairs is considered independently, and upstream cumulative plots are redefined as explained in Section 2.1.

3 TESTING

The methodology is tested using simulation. A network of five consecutive signalised intersections with stop-line detectors is considered (*see* Figure 7) and we define a route from intersection *A* to intersection *E*. Probe vehicles are randomly selected from vehicles traversing the route. For each travel time estimation period: a) Actual average travel time ($actual_i$) for the route is obtained from the simulated vehicles that traverse the complete route; b) CUPRITE (with approach R_C or R_E) provides the estimated average travel time ($estimated_i$). The performance of CUPRITE is evaluated in terms of accuracy (11), where initially, for each travel time estimation period absolute percentage error (APE) (9) is obtained. Thereafter, Mean Absolute Percentage Error (MAPE) (10) is defined.

$$APE_i = \left(\frac{|actual_i - estimated_i|}{actual_i}\right) * 100 \quad (9)$$

$$MAPE = \frac{\sum_{i=1 to N} APE_i}{N} \quad (10)$$

$$A_M(\%) = (100 - MAPE) \quad (11)$$

Here, first R_C and R_E estimation techniques are compared for flow F1 (where 90% of the flow at upstream traverses the route). Thereafter, the result of R_E application is provided for the following flow values:

1) F2: 50% of the flow at upstream traverses the route.
2) F3: 20% of the flow at upstream traverses the route.

Flow F1 is analogous to a route with major traffic flow. Flow F2 and F3 are analogous to the route where there is significant traffic in-flow and out-flow within the route. Two different case studies are performed:

1) Case M1: Here the comparison between the R_C and R_E approaches is performed for flow combinations F1 and for undersaturated (Case M1.U); and oversaturated traffic conditions (Case M1.O).
2) Case M2: Here different flow combinations (F1, F2 and F3) are analysed for R_E approach and compared with the average travel time from probes in each estimation period ("Probe-Only" method). A comparison of R_E with Probe-Only is made to evaluate the benefit of integrating cumulative plots with probes.

For R_C the components defined are through movements from *A* to *B*; *B* to *C*; *C* to *D*; and *D* to *E*. For R_E cumulative plots at upstream entrance at intersection *A* and downstream through exit at intersection *E* are considered.

3.1 Case M1

Figure 8 is a graph of accuracy versus fixed number of probes per estimated period (S_n) for undersaturated (case M1.U) and oversaturated (case M1.O) traffic conditions. During undersaturated traffic conditions, the virtual probe can be defined for each component and hence even in the absence of a real probe, accurate travel time can be obtained for R_C ($A_M > 96\%$ for $S_n = 0$) (*see* Figure 8*a*). During oversaturated traffic conditions, virtual probes are not considered and the accuracy for R_C increases with an increase in S_n (*see* Figure 8*b*).

Accuracy for R_C is slightly higher than that from R_E. As explained in Section 2.2, for R_C cumulative plots for each component of the route are to be accurately estimated, whereas for R_E cumulative plots only at the upstream entrance and downstream ext of the route are required. **Therefore, although R_C is more accurate and there are higher chances of getting probe for each component than the one traversing the complete path, detector data and signal timings are required for each component. R_E is simple to apply and data only at upstream and downstream points of the route is required, but the required probe should traverse the complete route, which could be a less frequent event.**

3.2 Case M2

In the previous section it is demonstrated that R_C performs better than R_E. Therefore, in this section we perform further testing using R_E. This provides a lower boundary for the performance as the approach R_C can slightly improve the accuracy. The results for the three different flows F1, F2 and F3 are presented in Figure 9.

1) With at least one probe per estimation interval the performance of CUPRITE is generally more than 95%, and increases with any increase in the number of probes. However, a significantly large number of probe vehicles are required to obtain comparable accuracy from the Probe-only method.
2) With less number of probes there is significant benefit to integrating cumulative plots with probe vehicles. For instance for S_n = 1 there is more than 5% improvement in accuracy. The availability of large numbers of probes per estimation period is quite rare and it demonstrates the significant benefit of integrating multiple data sources (detector data, signal timings and probe vehicle).

For the above analysis the "true" average travel time for the route is obtained by all the vehicles that traverse the complete route. For F3 (*see* Figure 9*c*) only 20% of the vehicles traverse the complete route. Therefore, for large S_n (>15) the accuracy from the *Probe-only* method is significantly higher. The above analysis indicates that CUPRITE can be applied for route travel time estimation for different flow combinations with implicit consideration of mid-route delay due to the presence of mid-route intersections.

4 VALIDATION

The methodology is validated on real data collected at Lucerne, Switzerland (Figure 10). The signal control at the site is equipped with an actuated signal controller VS-PLUS [35] that provides stop-line detector counts and signal timings. Individual vehicle data is obtained from manual number plate surveys from 3:00 pm to 6:00 pm on signalised intersections, indicated from *A* to *K* in Figure 10.

a) Traffic from *A* to *D* has significant flow from the freeway off ramp entering the city. It has a significant mid-link sink between intersection *C* and *D* where around 20% vehicles are lost to the side street to enter the city centre bypass;
b) Traffic from *D* to *I* passes through the city centre with bottlenecks at *F* and *I*. It also carries traffic to the railway station;
c) And traffic from *I* to *K* has no mid-link sink or source, but a significant amount of mid-link delay due to pedestrians. This route is along the lake side with a significant number of tourists.

This site characteristic includes detector counting errors; mixed traffic with buses; on-street bus stops; non conservation of traffic on the link due to side parking and side streets; significant mid-link delay due to pedestrian crossings; and urban links passing through the city centre.

CUPRITE is applied to estimate travel time for route A→F; route D→I; and route D→K. Each estimation period uses multiples of signal cycles, and accuracy during each period is defined using equations (9), (10) and (11) where actual travel time is from the aforementioned number plate survey. Both R_C and R_E are applied and compared. Figure 11*a*, *b* and *c* summarise the accuracy for three routes for R_C and R_E for S_n = 1, 2 and 3, respectively. It is observed that **accuracy from CUPRITE is more than 89% for different route combinations and increases by around 2% to 4% with an increase of S_n from 1 to 3, respectively.** Consistent with the testing results, **R_C performs better than R_E**.

Figure 12 represents the time series of average travel time from CUPRITE and from number plate survey data for R_E and R_C along the aforementioned routes for S_n=1. It can be seen that the **methodology has the potential to capture the time series of travel time and period to period travel time variations**. For instance, A→F route has increasing, decreasing and again increasing travel time for time from 15:30 to 16:00, 16:00 to 16:30 and 16:30 to 17:00, respectively. This is very well captured by the methodology.

5 CONCLUSION

One of the major limitations of existing travel time estimation models is that they estimate average travel time for the whole link. Generally, to estimate movement specific link travel time, penalties are added to the average link travel time. However, this cannot capture the dynamics of the traffic, and for real applications can result in significant error. This paper provides a methodology for robust and accurate exit movement specific travel time and its application for route travel time estimation. Two different approaches *Component* based and *Extreme* based are discussed for route travel time estimation.

The testing of the methodology for different flow combinations clearly indicates that the methodology can be applied for accurate estimation of route travel time with appropriate consideration of exit movement specific travel time. The validation of the methodology with real data from a typical urban network (with detector counting errors, mid-link sources and sinks, mixed traffic with buses, etc) provides confidence in the robustness of the methodology and its better network applicability. The results also demonstrate that the integration of different data sources has the potential to enhance the accuracy of the estimation. For instance, $S_n = 1$ there is more than 5% improvement in accuracy from the methodology than only from probes.

The application of the methodology provides detailed understanding of the network performance. For instance, excessive travel time for an exit movement can identify the critical movement at an intersection. The methodology accurately captures time series of travel time which can be used for developing an historical database of travel time. The latter is the basic requirement for travel time prediction. Hence the methodology can be extended by integrating it with prediction tools for accurate travel time prediction.

6 REFERENCES

[1] A. Dharia and H. Adeli, "Neural network model for rapid forecasting of freeway link travel time," *Engineering Applications of Artificial Intelligence,* vol. 16, pp. 607-613, 2003.

[2] D. H. Nam and D. R. Drew, "Traffic dynamics: Method for estimating freeway travel times in real time from flow measurements," *Journal of Transportation Engineering,* vol. 122, pp. 185-191, 1996.

[3] K. Jintanakul, L. Chu, and R. Jayakrishnan, "Bayesian mixture model for estimating freeway travel time distributions from small probe samples from multiple days," *Transportation Research Record,* vol. 2136, pp. 37-44, 2009.

[4] BPR, "Bureau of Public Roads: Traffic Assignment Manual," U. P. D. U.S. Dept. of Commerce, Washington D.C, Ed., ed, 1964.

[5] R. Akçelik, "A New Look at Davidson's Travel Time Function," *Traffic Engineering and Control,* vol. 19, pp. 459-463, 1978.

[6] P. Tisato, "Suggestions for an improved Davidson travel time function," *Australian road research,* vol. 21, pp. 85-100, June 1991 1991.

[7] H. Spiess, "Conical volume-delay functions," *Transportation Science,* vol. 24, pp. 153-158, 1990.

[8] F. V. Webster and B. M. Cobbe, *Traffic Signals*: Road Research Technical Paper No. 56, Her Majesty's Stationery Office, London, England., 1966.

[9] R. Akçelik, "Highway capacity delay forumula for signaliyed intersections," *ITE Journal (Institute of Transportation Engineers),* vol. 58, pp. 23-27, 1988.

[10] R. Akcelik and N. M. Rouphail, "Estimation of delays at traffic signals for variable demand conditions," *Transportation Research Part B: Methodological,* vol. 27, pp. 109-131, 1993.

[11] R. Akcelik and N. M. Rouphail, "Overflow queues and delays with random and platooned arrivals at signalized intersections," *Journal of Advanced Transportation,* vol. 28, pp. 227-251, 1994.

[12] R. Akçelik, "Travel time functions for transport planning purposes: Davidson's function, its time-dependent form and an alternative travel time function " *Australian Road Research* vol. 21, pp. 49-59., 1991.

[13] TRB, "Highway Capacity Manual," T. R. Board, Ed., ed. Washington, D.C.: National Research Council, 2000.

[14] TRB, "Highway Capacity Manual, Special Report 209," National Research Council, Washington D.C.1998.

[15] J. G. Wardrop, "Journey speed and flow in central urban areas," *Traffic Engineering and Control,* vol. 9, pp. 528-532, 1968.

[16] H. E. Gault, "An on-line measure of delay in road traffic computer controlled systems," *Traffic Engineering and ControL,* vol. 22 pp. 384-389, 1981.

[17] C. P. Young, "A relationship between vehicle detector occupancy and delay at signal-controlled junctions," *Traffic Engineering and Control,* vol. 29, pp. 131-134, 1988.

[18] V. P. Sisiopiku and N. M. Rouphail, "Toward the use of detector output for arterial link travel time estimation: a literature review," *Transportation Research Record,* pp. 158-165, 1994.

[19] V. P. Sisiopiku, N. M. Rouphail, and A. Santiago, "Analysis of correlation between arterial travel time and detector data from simulation and field studies," *Transportation Research Record,* pp. 166-173, 1994.

[20] H. M. Zhang, "Link-journey-speed model for arterial traffic," *Transportation Research Record,* pp. 109-115, 1999.

[21] S. Robinson and J. W. Polak, "Modeling Urban Link Travel Time with Inductive Loop Detector Data by Using the k-NN Method," *Transportation Research Record,* vol. 1935, pp. 47-56, 2005.

[22] P. V. Palacharla and P. C. Nelson, "Application of fuzzy logic and neural networks for dynamic travel time estimation," *International Transactions in Operational Research,* vol. 6 (1), pp. 145-160, 1999.

[23] H. Liu, H. J. Van Zuylen, H. Van Lint, Y. Chen, and K. Zhang, "Prediction of urban travel times with intersection delays," in *IEEE Conference on Intelligent Transportation Systems, Proceedings, ITSC,* Vienna, 2005, pp. 1062-1067.

[24] B. R. Hellinga and L. Fu, "Reducing bias in probe-based arterial link travel time estimates," *Transportation Research Part C: Emerging Technologies,* vol. 10, pp. 257-273, 2002.

[25] R. Long Cheu, C. Xie, and D. H. Lee, "Probe vehicle population and sample size for arterial speed estimation," *Computer-Aided Civil and Infrastructure Engineering,* vol. 17, pp. 53-60, 2002.

[26] K. Srinivasan and P. Jovanis, "Determination of Number of Probe Vehicles Required for Reliable Travel Time Measurement in Urban Network," *Transportation Research Record: Journal of the Transportation Research Board,* pp. 15-22, 1996.

[27] N. E. El Faouzi, "Data fusion in road traffic engineering: An overview," in *Proceedings of SPIE - The International Society for Optical Engineering*, Orlando, FL, 2004, pp. 360-371.

[28] D. J. Dailey, P. Harn, and P.-J. Lin, "ITS Data Fusion," ITS Research Program, University of Washington http://www.its.washington.edu/pubs/fusion_report.pdf (Last accessed January 2010)1996.

[29] S. Berka, A. Tarko, N. M. Rouphail, V. P. Sisiopiku, and D.-H. Lee, "Data fusion algorithm for ADVANCE Release 2.0," *Advance Working Paper Series, No. 48, University of Illinois at Chicago, Chicago, IL,* 1995.

[30] K. Choi and Y. Chung, "A data fusion algorithm for estimating link travel time," *ITS Journal: Intelligent Transportation Systems Journal,* vol. 7, pp. 235-260, 2002.

[31] C. Xie, R. L. Cheu, and D. H. Lee, "Improving arterial link travel time estimation by data fusion," *83rd Annual Meeting of the Transportation Research Board,* 2004.

[32] C. F. Daganzo, *Fundamentals of Transportation and Traffic Operations*: Pergamon, Oxford, 1997.

[33] A. Bhaskar, E. Chung, and A.-G. Dumont, "Estimation of Travel Time on Urban Networks with Midlink Sources and Sinks," *Transportation Research Record: Journal of the Transportation Research Board,* vol. 2121, pp. 41-54, 2009.

[34] A. Bhaskar, E. Chung, and A.-G. Dumont, "Analysis for the Use of Cumulative Plots for Travel Time Estimation on Signalized Network," *International Journal of Intelligent Transportation Systems Research,* vol. 8, pp. 151-163, 2010.

[35] VS-PLUS. *http://www.vs-plus.com/e/vsintro.htm (last accessed July 2011).*

7 LIST OF FIGURES

Figure 1: *a, c* and *d*) Illustration of an urban link with different flow and geometric configurations; *b*) time series of real travel time for different exit movements from a signalised link at Luzern, Switzerland. 14
Figure 2: Classical analytical procedure and its vulnerability to relative deviation (RD) amongst the plots. 15
Figure 3: CUPRITE architecture for link-movement specific travel time estimation. 16
Figure 4: a) Vertical scaling of $U_T(t)$ for initial estimate of $U_m(t)$; b) Integrating $U_m(t)$ with probes. 17
Figure 5: Example of the methodology for estimation of upstream cumulative plot for each exit turning movement. 18
Figure 6: Example for RC and RE. 19
Figure 7: Network for CUPRITE testing for route travel time estimation. 20
Figure 8: Case Study a) M1.U and b) M1.O for Flow = F1 versus S_n. 21
Figure 9: R_E and Probe-only performance versus S_n): a) F1; b) F2 and c) F3. 22
Figure 10: Study area (Luzern, Switzerland) 23
Figure 11: Route travel time validation for routes on Luzern data. 24
Figure 12: Time series of estimated and observed travel time on different routes at Luzern 25

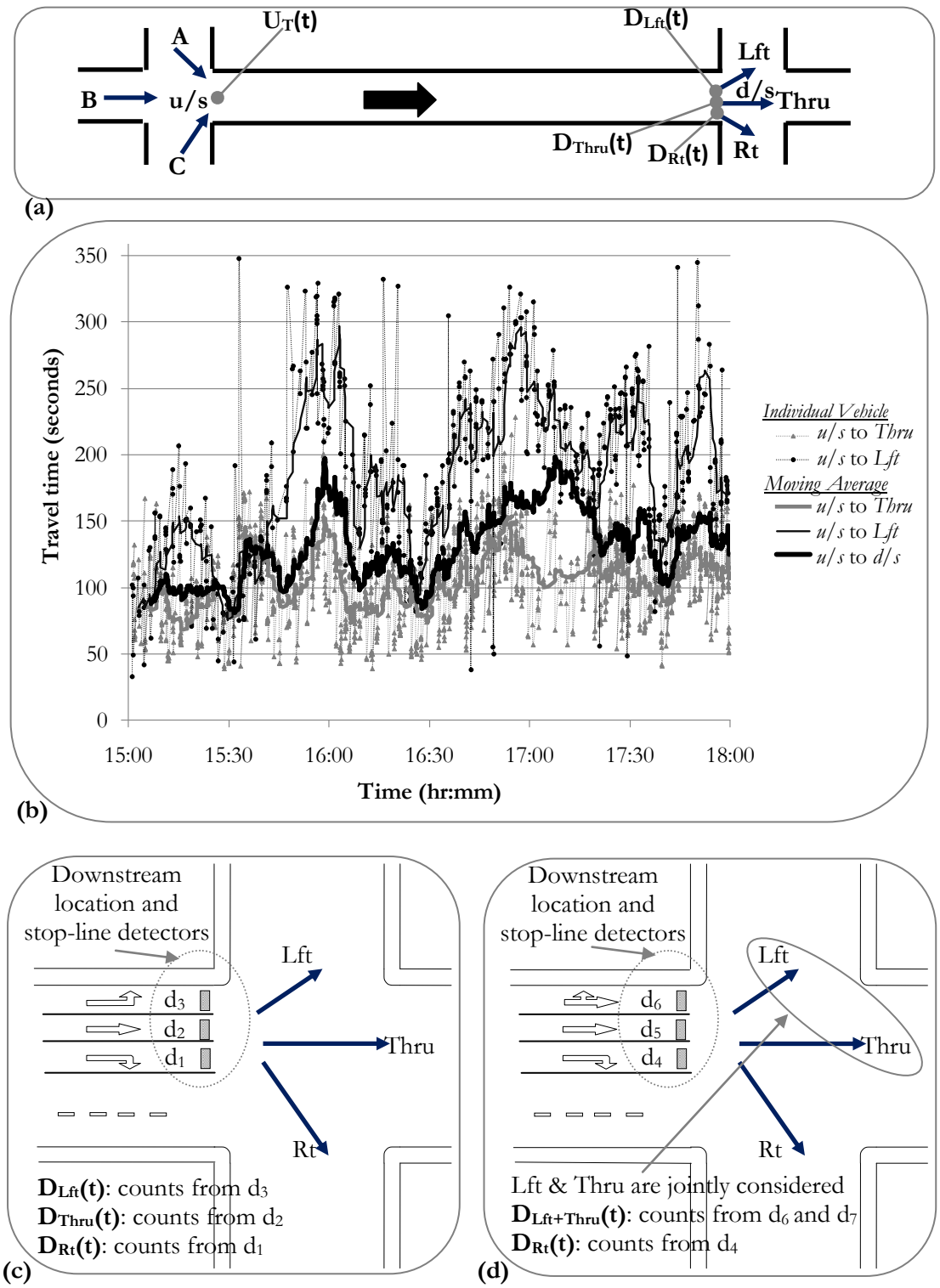

Figure 1: *a, c* and *d*) Illustration of an urban link with different flow and geometric configurations; *b*) time series of real travel time for different exit movements from a signalised link at Luzern, Switzerland.

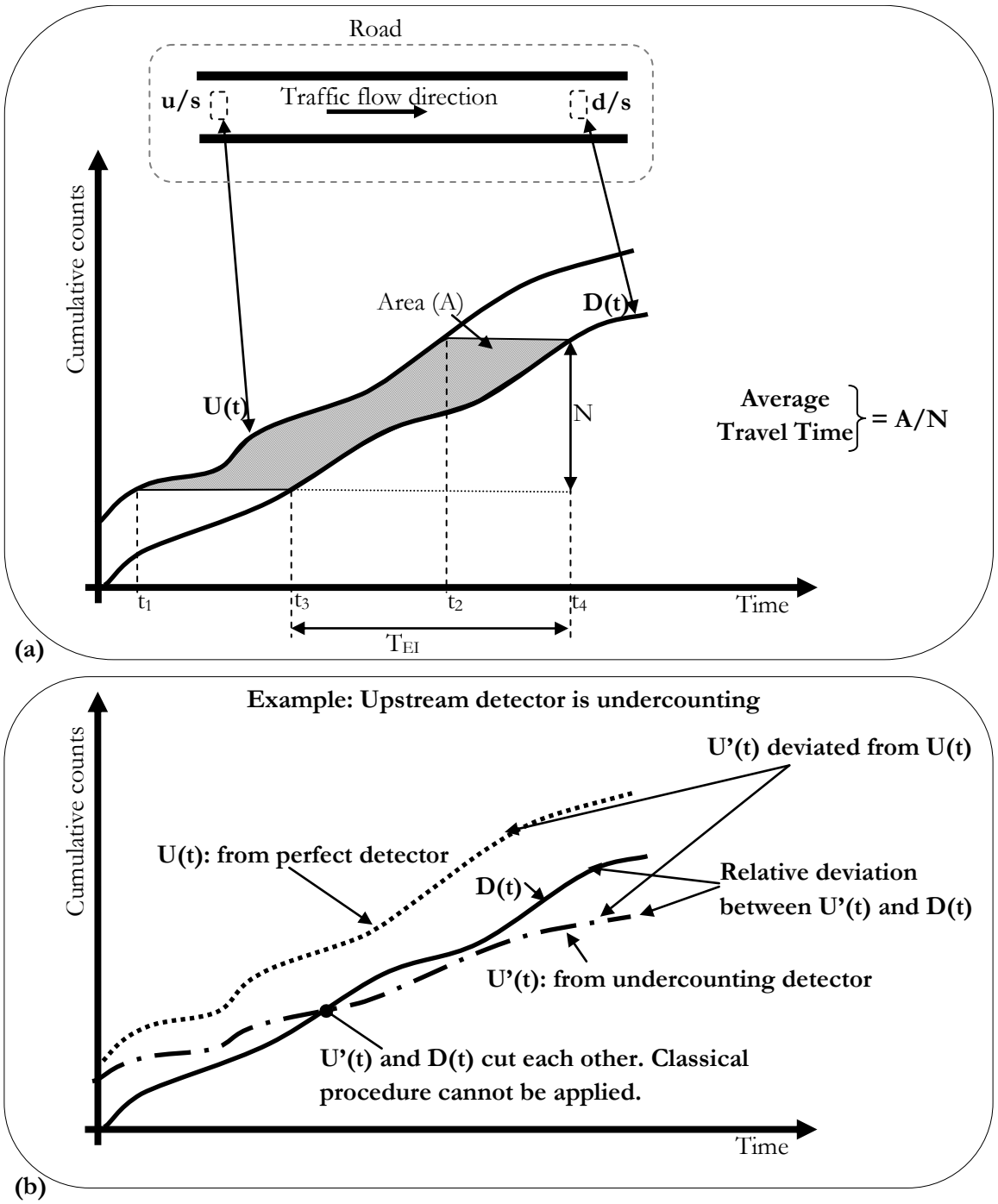

Figure 2: Classical analytical procedure and its vulnerability to relative deviation (RD) amongst the plots.

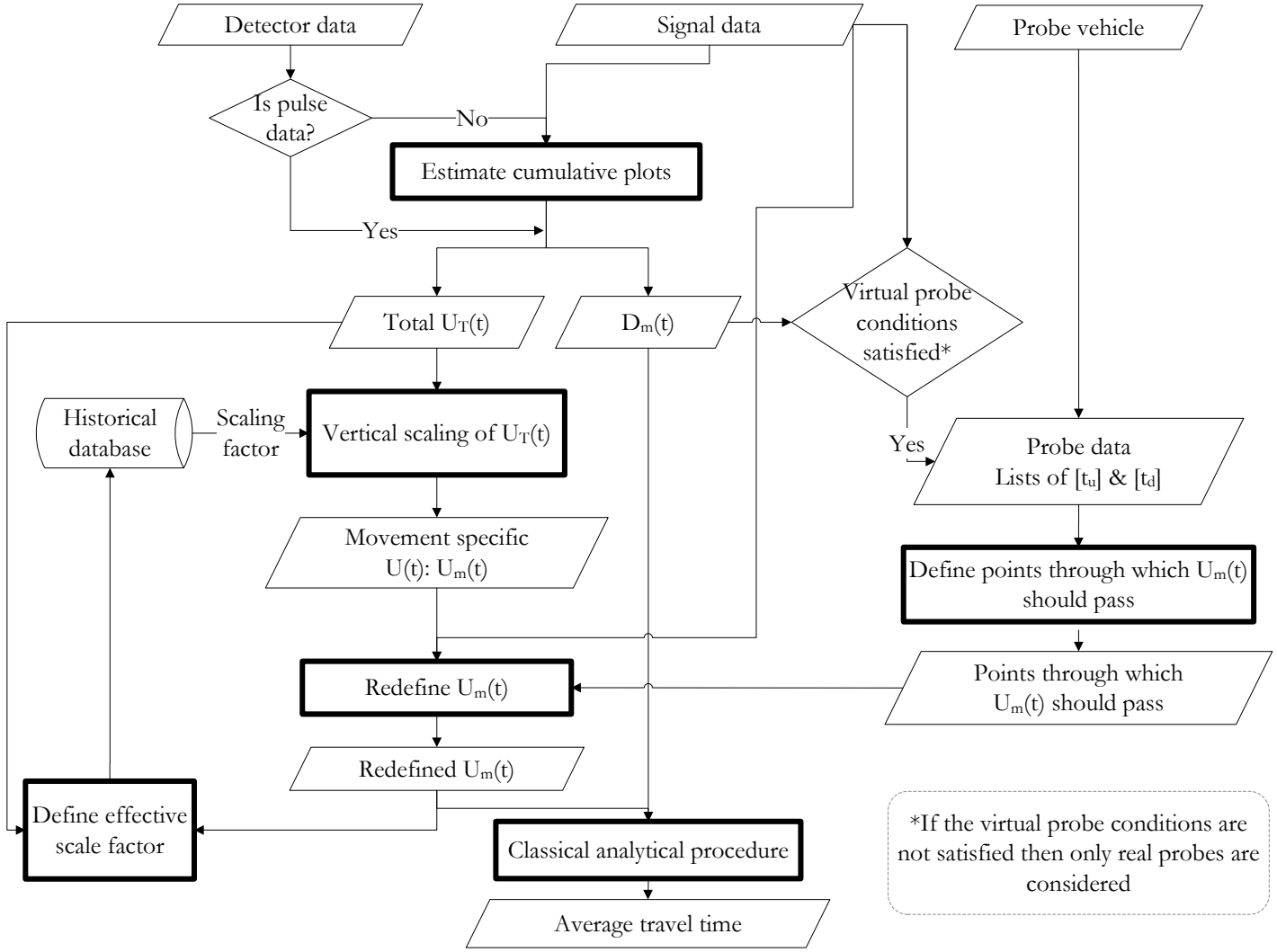

Figure 3: CUPRITE architecture for link-movement specific travel time estimation.

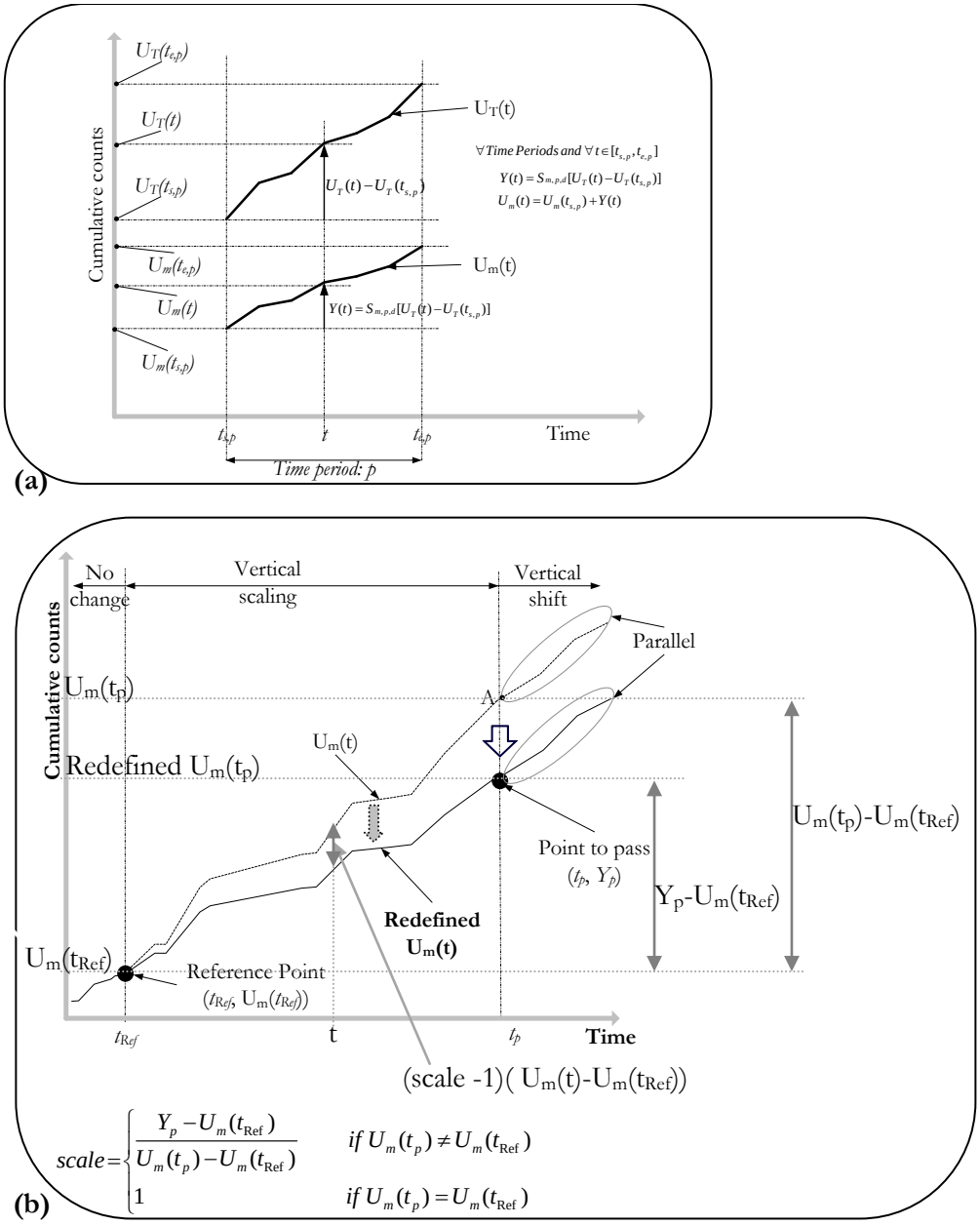

$$scale = \begin{cases} \dfrac{Y_p - U_m(t_{\text{Ref}})}{U_m(t_p) - U_m(t_{\text{Ref}})} & \text{if } U_m(t_p) \neq U_m(t_{\text{Ref}}) \\ 1 & \text{if } U_m(t_p) = U_m(t_{\text{Ref}}) \end{cases}$$

Figure 4: a) Vertical scaling of $U_T(t)$ for initial estimate of $U_m(t)$; b) Integrating $U_m(t)$ with probes.

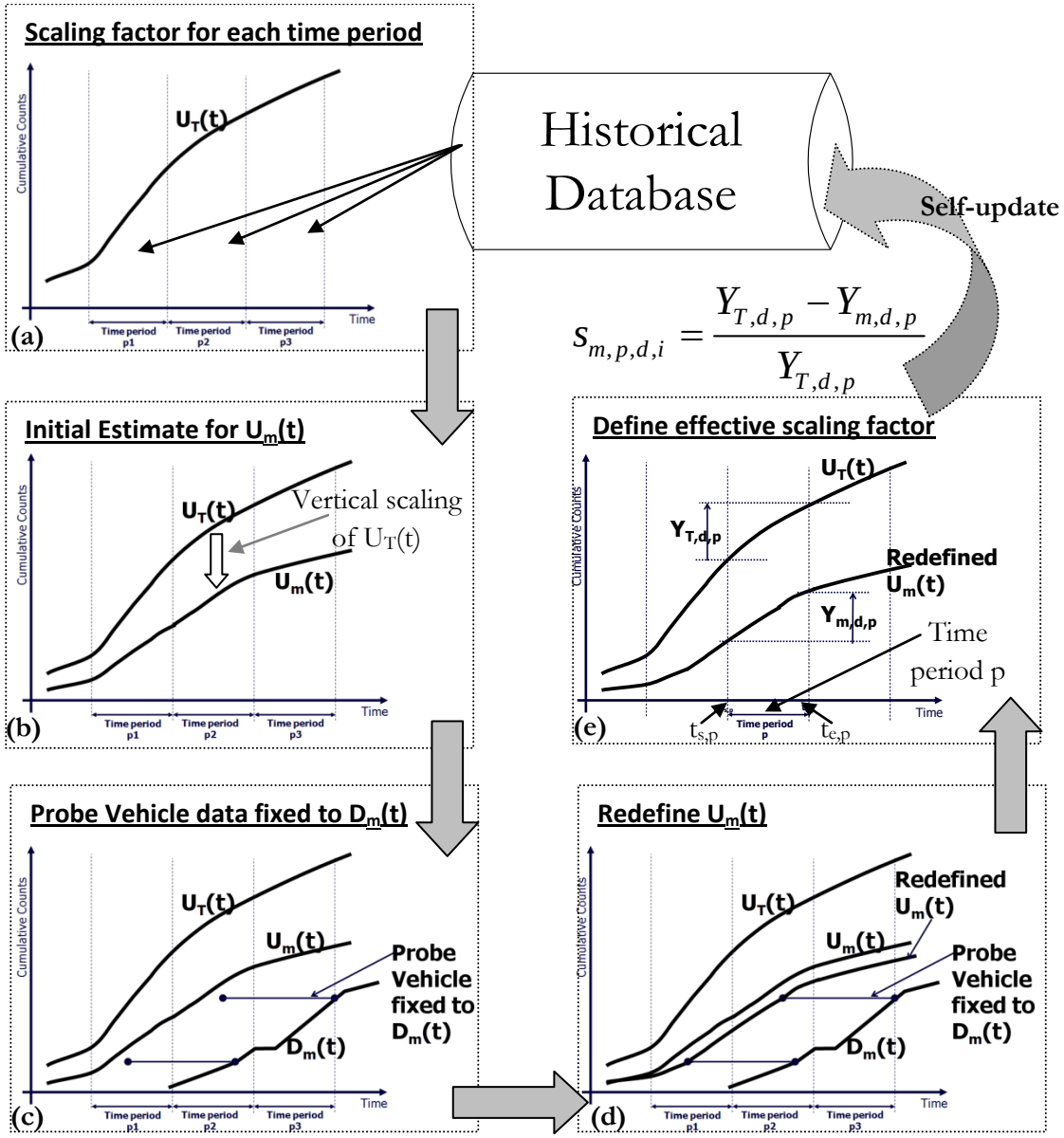

Figure 5: Example of the methodology for estimation of upstream cumulative plot for each exit turning movement.

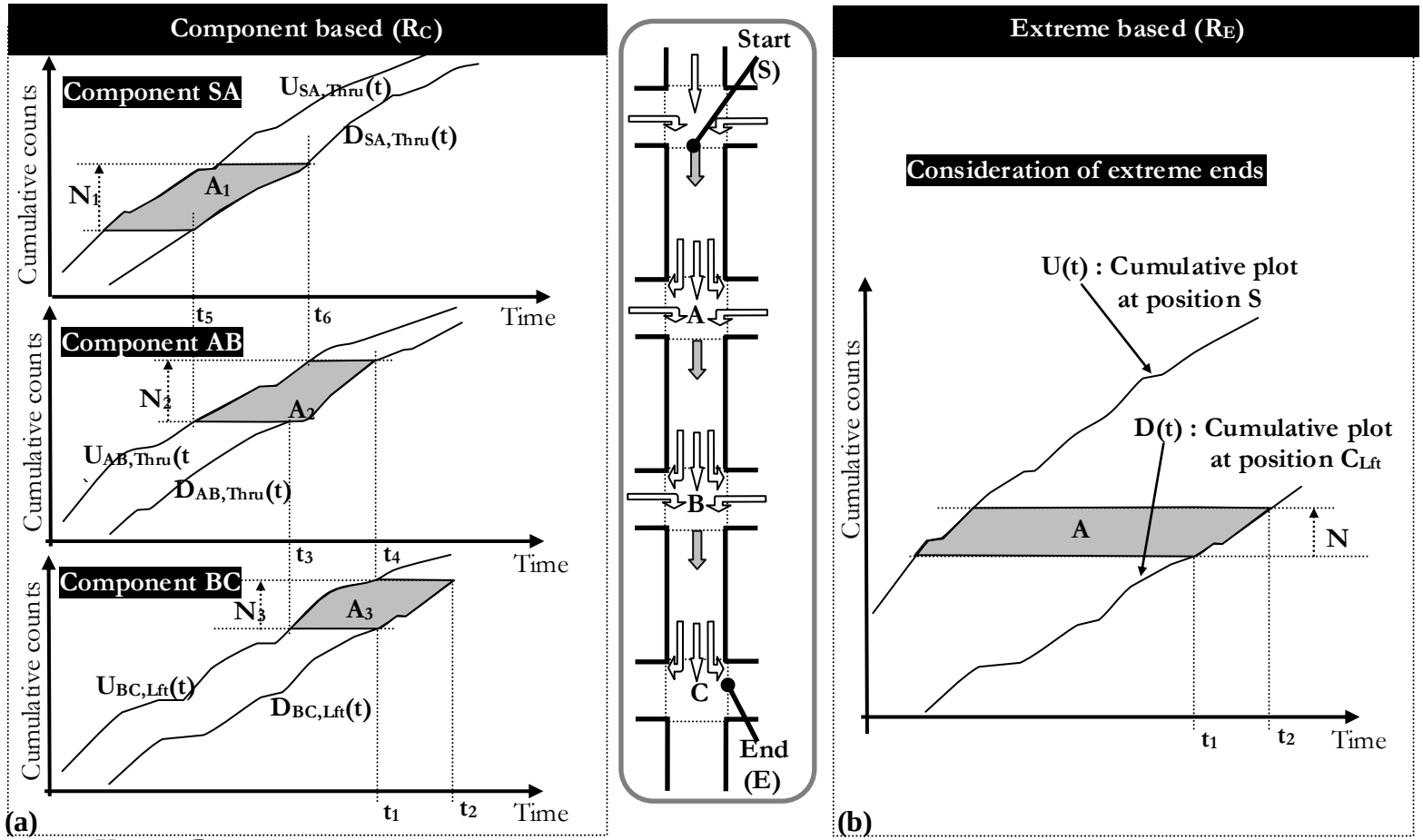

$t_3 = U_{BC,Lft}^{-1}(D_{BC,Lft}(t_1))$
$t_4 = U_{BC,Lft}^{-1}(D_{BC,Lft}(t_2))$
$t_5 = U_{AB,Thru}^{-1}(D_{AB,Thru}(t_3))$
$t_6 = U_{AB,Thru}^{-1}(D_{AB,Thru}(t_4))$

$TT_i = A_i/N_i$
Route $TT = \sum TT_i$ $(i=1,2,3)$

Route $TT = A/N$

Figure 6: Example for RC and RE.

1

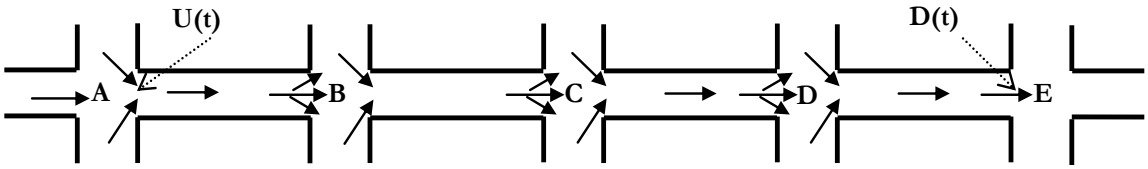

F1 : 90% of the vehicles in U(t) are also in D(t)
F2 : 50% of the vehicles in U(t) are also in D(t)
F3 : 20% of the vehicles in U(t) are also in D(t)

- All intersections are signalized
- All links are two lanes, with separate left and right movement lane.
- Length of each link is approx 500 m

2
3 **Figure 7: Network for CUPRITE testing for route travel time estimation.**
4
5

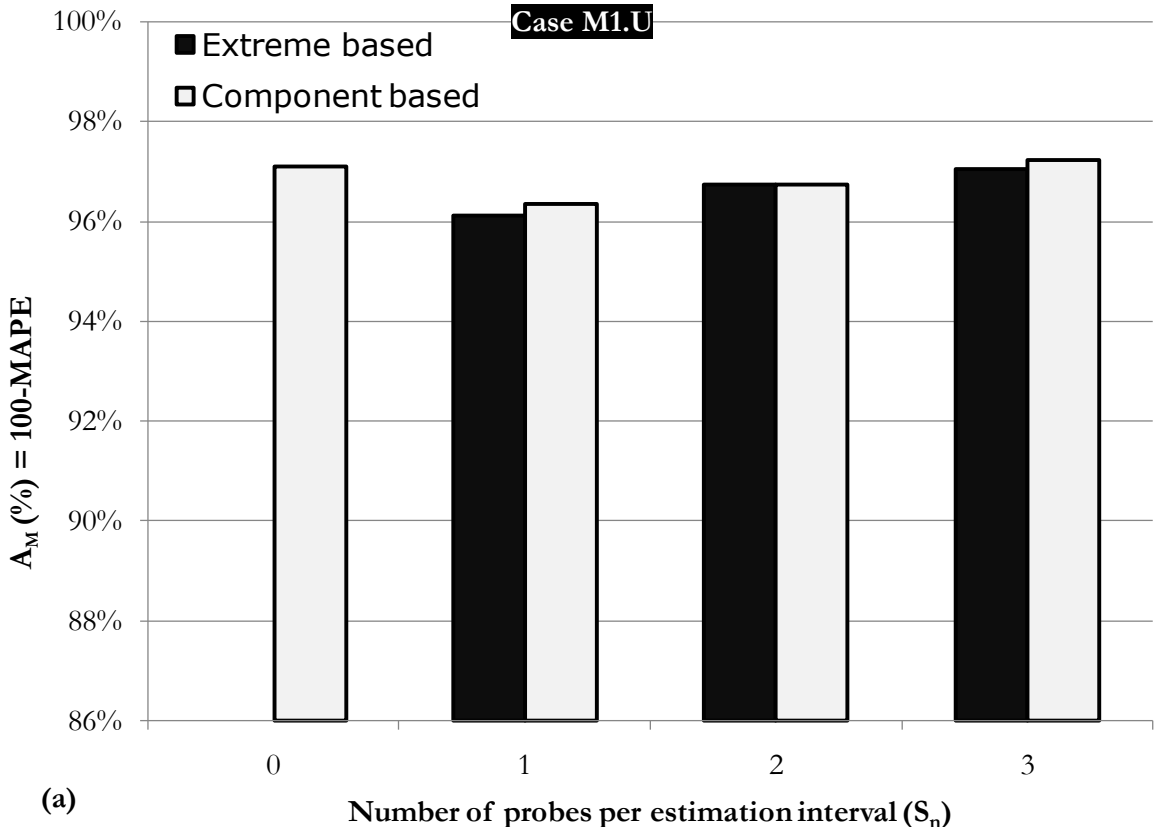

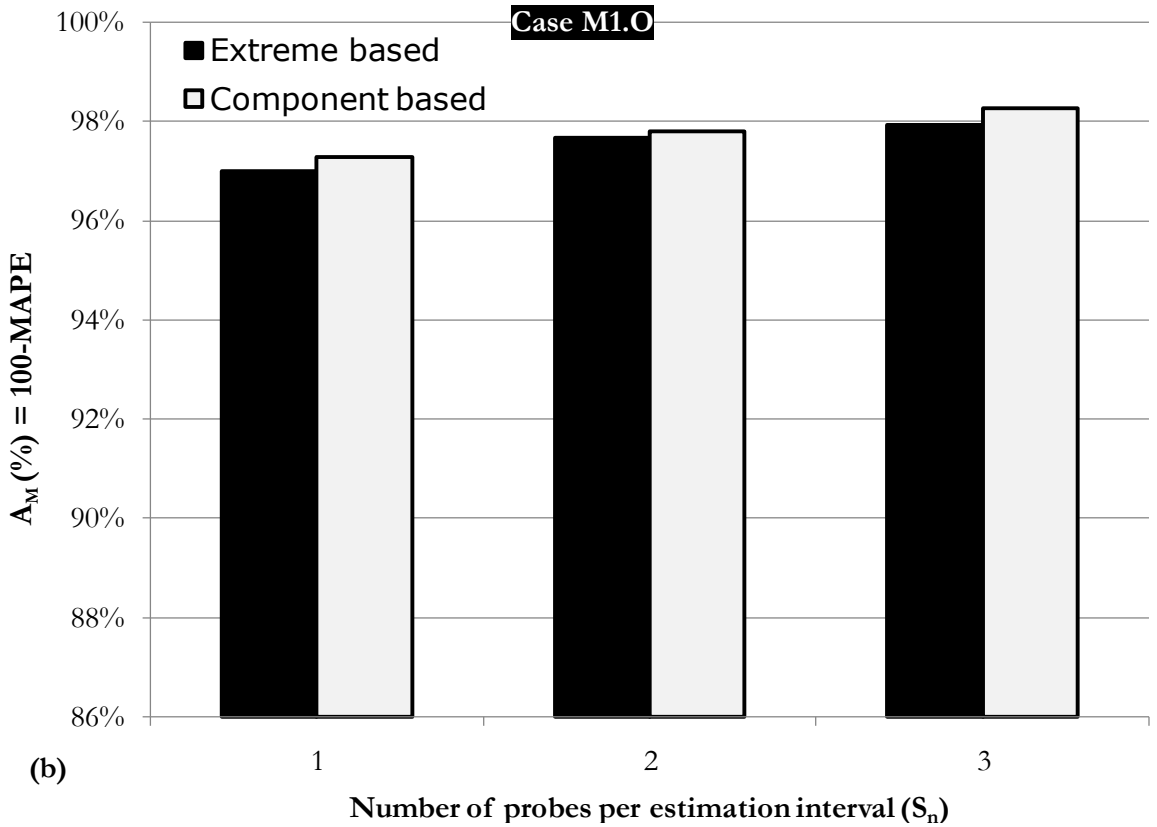

Figure 8: Case Study a) M1.U and b) M1.O for Flow = F1 versus S_n.

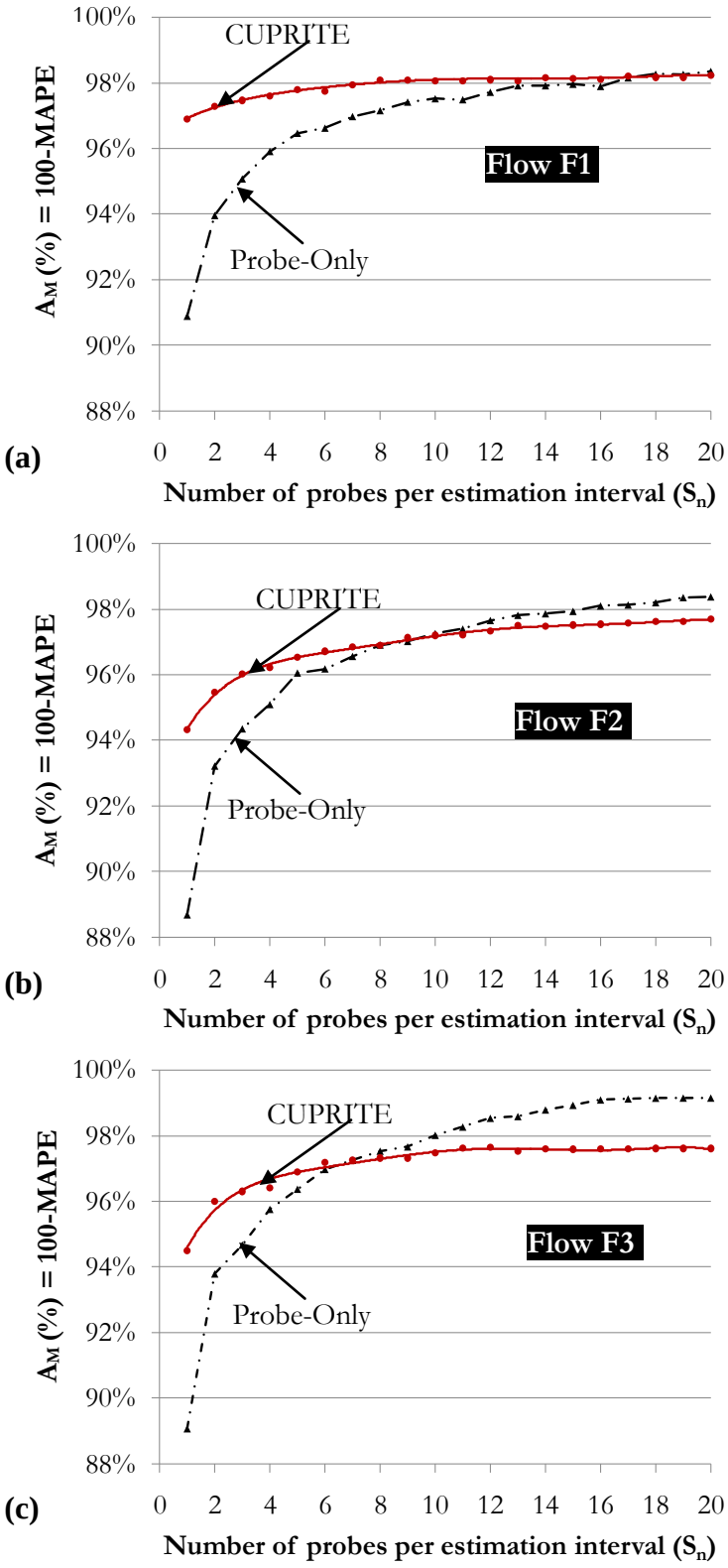

Figure 9: R_E and Probe-only performance versus S_n): a) F1; b) F2 and c) F3.

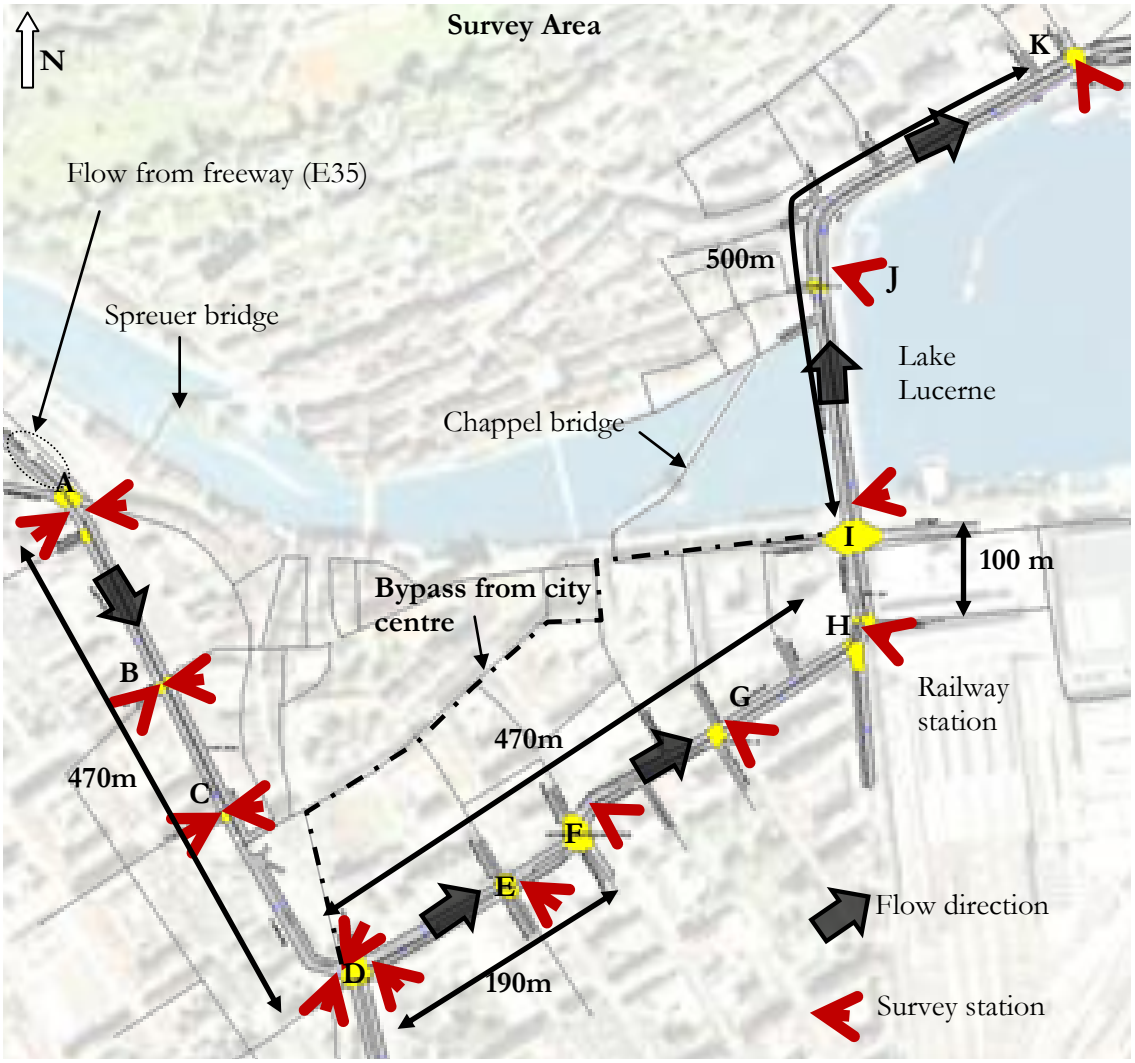

Figure 10: Study area (Luzern, Switzerland)

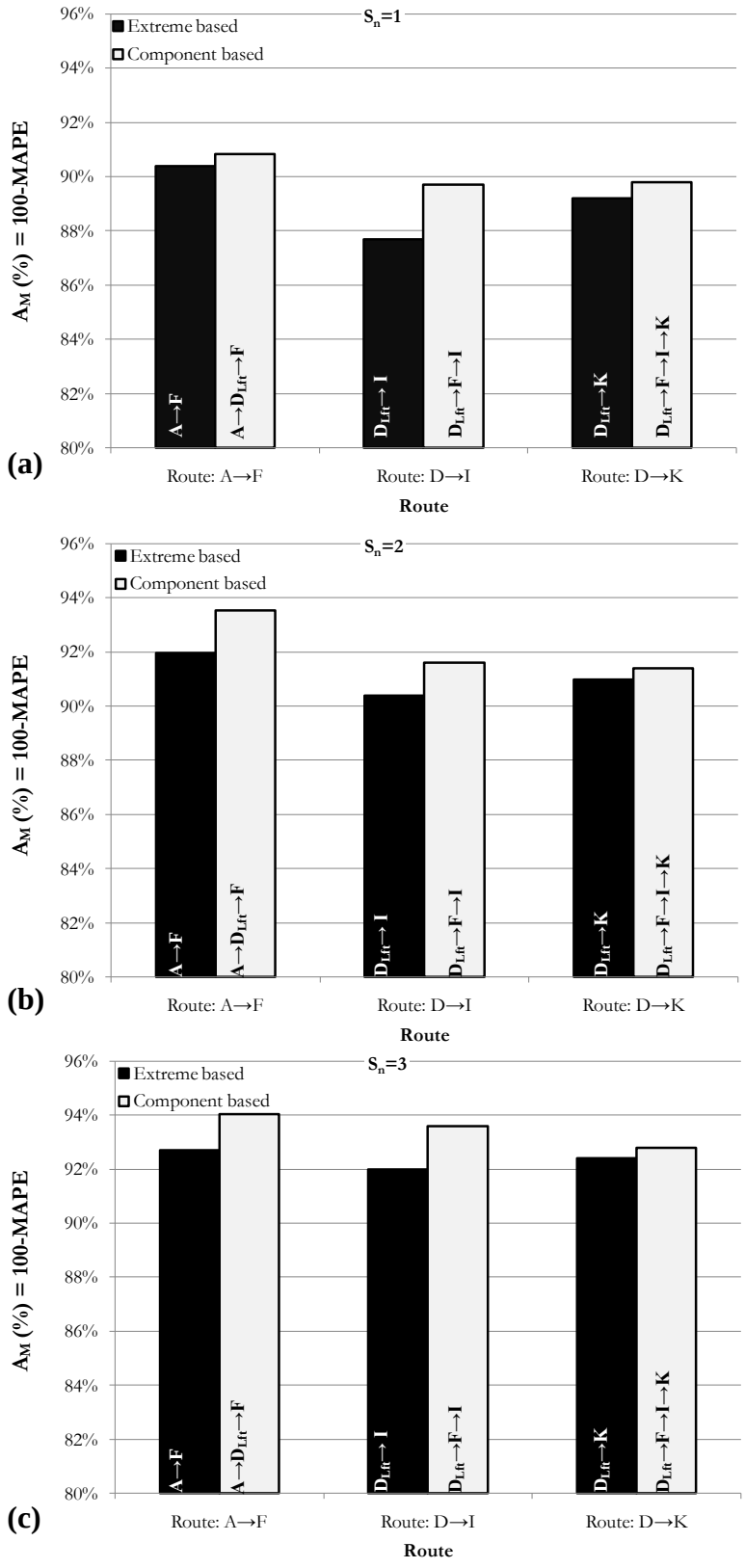

Figure 11: Route travel time validation for routes on Luzern data.

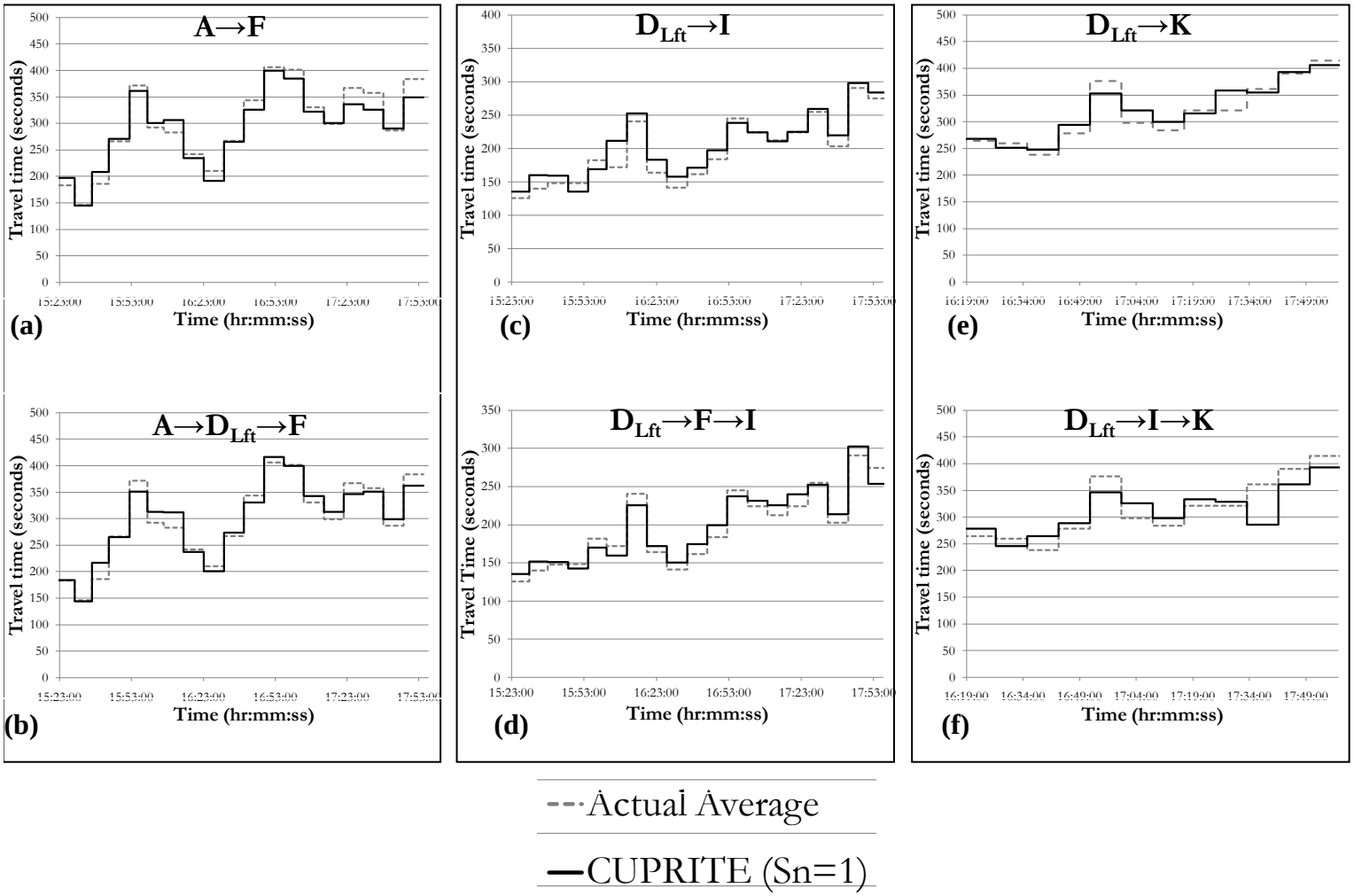

Figure 12: Time series of estimated and observed travel time on different routes at Luzern

1